Proc. Natl. Acad. Sci. USA
Vol. 91, pp. 4160–4164, May 1994
Biochemistry

Structure of a mispaired RNA double helix at 1.6-Å resolution and implications for the prediction of RNA secondary structure

(crystal structure/C·U base pair/G·U base pair/T·T base pair/hydrogen bond)

WILLIAM B. T. CRUSE†, PEDRO SALUDJIAN‡, EWA BIALA†, PETER STRAZEWSKI†, THIERRY PRANGÉ‡§, AND OLGA KENNARD†

†Cambridge Crystallographic Data Centre, 12 Union Road, Cambridge CB2 1EZ, United Kingdom; ‡Chimie Structurale Biomoléculaire (URA 1430 Centre National de la Recherche Scientifique) rue M. Cachin, 93012-BOBIGNY Cedex, France; and §Laboratoire pour l'Utilisation du Rayonnement Electromagnetique, Bat. 209d, Université Paris-Sud, 91405-ORSAY Cedex, France

Communicated by Arnold Burgen, December 30, 1993

ABSTRACT **The nonamer r(GCUUCGGC)d^{Br}U, where d^{Br}U is 5-bromo-2′-deoxyuridine, contains the tetraloop sequence UUCG. It crystallizes in the presence of $Rh(NH_3)_6Cl_3$. In solution the oligomer is expected to form a hairpin loop but the x-ray structure analysis, to a resolution of 1.6 Å, indicates an eight-base-pair A-RNA duplex containing a central block of two G·U and two C·U pairs. Self-pairs which approximate to Watson–Crick geometry are also formed in the extended crystal structure between symmetry-related ^{Br}U residues and are part of infinite double-helical stacks. The G·U pair is a wobble base pair analogous to the G·T pair found in DNA fragments. The C·U mismatch involves one hydrogen-bonded contact between the bases and a bridging water molecule which ensures a good fit of the base pair in the RNA helix. The ^{Br}U·^{Br}U pair is held by two hydrogen bonds in an orientation which is compatible with duplex geometry. The structure observed within the crystal has some parallels with the structure of globular RNAs, and the presence of stable, noncanonical base pairs has implications for the prediction of RNA secondary structure.**

Tertiary structure is essential to the biological function of many single-stranded RNAs. Base pairing between complementary segments in a sequence generates a series of double-helical stems that connect unpaired regions or loops. These can fold further into compact assemblies stabilized by additional hydrogen bonds and by hydrophobic and electrostatic interactions (1). The various levels of structural order are most completely characterized in tRNAs, for which a number of crystal structures have been determined (2–4). In the case of larger and more complex RNA species, including ribosomal components and RNase P, present understanding of secondary structure relies heavily on assumptions about the relative stabilities of possible base-pairing arrangements (5). These follow the specificities of adenine for uracil and guanine for cytosine observed in both ribonucleotides and deoxyribonucleotides during replication and transcription and are also mirrored in the experimentally measured stabilities of short oligonucleotide duplexes. Although the double helix is a central feature of these systems, none is a conspicuously direct model of the environment within a globular RNA structure.

The present analysis of an RNA double helix is the second to be reported for an oligonucleotide containing a "tetraloop" sequence. Tetraloops are common in natural single-stranded RNA and, although the stems of such structural elements are variable, the unpaired regions are found to be tetranucleotides of mainly two types: a group with the general sequence r(GNRA) and the specific r(UUCG). Examples of both classes have been examined extensively in solution, where they exist as monomeric, thermally stable, looped species which parallel the behavior of the parent sequences in RNA of higher molecular weight (6, 7).

In crystals of both the present sequence and a dodecamer studied by Holbrook *et al.* (8), where r(UUCG) is embedded in self-complementary sequences, duplexes are formed. Four adjacent base pairs at their centers are of the noncanonical types U·G and U·C. These are accommodated with remarkably little distortion of the canonical A-RNA sugar-phosphate backbone, even in the case of the pyrimidine–pyrimidine pair, where inclusion of a water molecule in interbase hydrogen-bonding allows the glycosidic bonds to adopt similar relative orientations to those in a Watson–Crick pair. The analysis demonstrates that base–base complementarity within the stable RNA double helix is not invariably restricted to A·U and G·C, especially when the duplex is stabilized by external interactions. In this respect, the environments of RNA in globular structures and in crystals may be considered analogous, and the present result should be taken into account when secondary structures are predicted.¶

MATERIALS AND METHODS

Synthesis, Crystallization, and Data Collection. The sequence r(GCUUCGGC)d^{Br}U was chosen because it includes the tetraloop sequence and a short stem potentially stabilized by triply hydrogen-bonded base pairs. A dangling bromodeoxyuridine was included at the 3′ end in the hope that this might aid crystallization. The oligomer was prepared by automated solid-phase synthesis (Applied Biosystems model 381A) using 2′-*t*-butyldimethylsilyl-protected phosphoramidite monomers (Peninsula Laboratories). Purification was by ion-exchange and reverse-phase HPLC. The nonamer was crystallized as the ammonium salt at 4°C from sitting drops of 60 μl by reverse vapor diffusion against 40% aqueous 2-methyl-2,4-pentanediol. Each droplet contained 0.1 mg of the nonamer in 20 mM lithium cacodylate (pH 6.3), with 6–10 mM $Rh(NH_3)_6Cl_3$ or $Ir(NH_3)_6Cl_3$. Thin, elongated plates appeared within 6 hr, growing to an optimal size of 0.3 mm × 0.5 mm × 0.05 mm over a period of 7–14 days. The RNA complex was unusually stable to cooling and heating and was reversibly crystalline. The crystals were monoclinic with unit cell dimensions a = 53.8 Å, b = 19.40 Å, c = 50.14 Å, β = 109.9° and space group $C2$. They diffracted to a resolution of better than 1.5 Å. There are two nonamer strands in the

The publication costs of this article were defrayed in part by page charge payment. This article must therefore be hereby marked "*advertisement*" in accordance with 18 U.S.C. §1734 solely to indicate this fact.

¶The atomic coordinates and structure factors have been deposited in the Protein Data Bank, Chemistry Department, Brookhaven National Laboratory, Upton, NY 11973 (reference 1650, R1650SF).

asymmetric unit ($Z = 8$), four rhodium (or iridium) hexammine cations, and 55 located water molecules.

Intensity data were collected with the rhodium and iridium complexes at the Laboratoire pour l'Utilisation du Rayonnement Electromagnetique Synchrotron Facility, Orsay, France, on the MAR Research image-plate system. The nominal resolution was 1.6 Å for x-rays of wavelength 0.9 Å. Several data sets for each derivative were also obtained on the Enraf–Nonius FAST system to a resolution of 1.95 Å (wavelength, 1.54 Å). For the rhodium complex they were merged as a unique set of 6424 structure factors, with 6093 above the 2σ level.

Structure Analysis. The structure was solved in several stages. First, the heavy atoms were located from difference Patterson maps between the isomorphous iridium and rhodium complexes and from anomalous difference Patterson maps for each derivative alone using the FAST data set. Two heavy-atom sites were located and refined by using only the iridium data set.

The next stage used the molecular replacement program AMORE (9). It is possible with this program to build a model from several structural elements, rotate and translate each independently, and test all possible combinations of solutions.

The present analysis used three elements. A translational search confirmed the heavy-atom positions. Next a model was constructed from the coordinates of the central region of eight bases of the dodecamer sequence r(GGACUUCG-GUCC) (8), kindly provided by S. R. Holbrook. The terminal bases were changed on a graphics system for the correct sequence (A changed to G and U to C at positions 1 and 8). When the model was constructed the bases were labeled G^1 to $^{Br}U^9$ in the 5′- to -3′ direction on strand 1, and G^{10} to $^{Br}U^{18}$ in the 5′- to -3′ direction on the second strand. A double helix was generated from this single strand by a twofold symmetry operator. The second strand could have been located from peaks obtained by AMORE, but introduction of symmetry speeded up convergence.

Finally, one of the ^{Br}U residues was added to the model independently of the double helix already located, by using published coordinates (10). The second ^{Br}U was expected to show up in the searches but this position, as subsequently discovered, was disordered and only one ^{Br}U peak appeared.

By using the optimal solutions from AMORE the different parts of the model were linked together and checked for unfavorable interactions. The complete ensemble was refined as a rigid body and converged to an R factor of 42% with 1547 structure factors at a resolution of 2.1 Å.

Refinement was continued with XPLOR (11) using data between 10 and 1.6 Å. $2F_o - F_c$ and $F_o - F_c$ Fourier maps were calculated and examined on a graphics system. The second ^{Br}U was found in two disordered positions around the twofold axis at the origin. These were included in the refinement with 50% occupancy, as well as two further minor rhodium positions with partial occupancy. Water molecules were gradually included on the basis of reasonable bond distances (2.6–3.1 Å) and angles (90–130°) toward polar atoms of the duplex or neighboring solvent positions. The refinement converged to a R value of 18.0% for 6093 structure factors above 2σ with 55 water molecules. The atomic displacement parameters (B values) at the double-helical regions are 5–10 Å^2. Those of the disordered ^{Br}U are 24 and 29 Å^2, while B for water oxygens ranges from 6 to 30 Å^2. A detailed report of the methods used in the analysis will be published elsewhere.

RESULTS

Structure of r(GCUUCGGC)d^{Br}U. The asymmetric unit of the crystal structure consists of two chemically equivalent strands of the nonamer r(GCUUCGGC)d^{Br}U. The RNA portions form an antiparallel double helix with four Watson–Crick base pairs and four mismatched base pairs, U^3·G^{15}, U^4·C^{14}, C^5·U^{13}, and G^6·U^{12}. The discovery that the molecule crystallizes as a duplex was unexpected, since sequences with self-complementary elements separated by the tetraloop motif r(UUCG) typically form looped structures in solution. A similar double helix was found in the RNA dodecamer by Holbrook *et al.* (8).

The double-helical region has almost perfect twofold symmetry, although the two strands were allowed to refine independently. The symmetry is manifest both in the equivalence of the various helical parameters (Table 1) and from a least-squares superposition calculation. With all atoms other than those of the two ^{Br}U residues the mean deviation between the two strands is 0.68 Å.

The principal deviation is at the α and γ torsion angles between G^{15} and G^{16} on strand 2, which changes the orientation around the C4′—C5′ bond between two *gauche* positions. This may well be due to the effect of Rh^{21}, which is in the major groove, close to G^{16} and G^{17} as described in the next section.

The double helix is generally of the A-RNA type with individual torsion angles within the ranges typical of this form. The average rise per residue is 2.8 Å and the helix rotation is 37.4°, giving 9.63 base pairs per turn. The corresponding values for the RNA dodecamer structure are 2.93 Å, 32.1°, and 11.2; and for the canonical A-RNA; 2.81 Å, 32.7°, and 11.0. The sugar conformation is C3′-*endo* throughout with pseudorotation angles between 14° and −2° except for the deoxyribose of $^{Br}U^9$ ($P = 21°$).

The ^{Br}U residues are not related by the twofold symmetry of the duplex. $^{Br}U^9$ at the 3′- end of strand 1 is directed away from the helix. $^{Br}U^{18}$ on strand 2 is disordered between two positions both directed to the helical core as discussed below.

G·U Mismatch. The G·U base pairs identified in the present analysis are shown in Fig. 1, superimposed on the electron density map at 1.6-Å resolution. The analogous G·T base pairs have been well characterized in crystal structures of DNA fragments in A, B, and Z conformations (12); G·U pairs themselves have been observed in stem regions of tRNA (2–4) and the RNA dodecamer (8). In all these structures the mismatched base pairs are of the "wobble" type (Fig. 1) with one hydrogen bond between N3 of the pyrimidine and O6(G) and a second between O2 of pyrimidine and N1(G). Distances in the nonamer are as follows: N3(U^3) · · · O6(G^{15}), 2.90 Å; O2(U^3) · · · N1(G^{15}), 2.79 Å; corresponding distances in the U^{12}·G^6 base pair are 2.77 and 2.70 Å. The purine and pyrimidine components are displaced towards the major and minor grooves, respectively. Widespread preference shown for this mode of pairing between G and U (or T) is strong

Table 1. Characteristics of the base pairs in r(GCUUCGGC)d^{Br}U

Base pair	Propellor twist, degrees	C1′–C1′ distance, Å	c1, degrees	c2, degrees
G^1·C^{17}	−11.4	10.38	53.6	57.0
C^2·G^{16}	−9.6	10.44	55.2	56.5
U^3·G^{15}	−6.8	10.52	67.8	42.6
U^4·C^{14}	1.4	12.09	30.6	36.4
C^5·U^{13}	3.0	11.92	38.9	33.1
G^6·U^{12}	−11.75	10.43	42.8	67.8
G^7·C^{11}	−9.6	10.63	55.1	54.7
C^8·G^{10}	−5.2	10.62	57.1	51.5

c1 and c2, angles between the glycosidic bond C1′ → N1 and C1′ → C1′ vectors for bases in strands 1 and 2, respectively, calculated with the program NEWHEL91 (provided by R. E. Dickerson, University of California, Los Angeles).

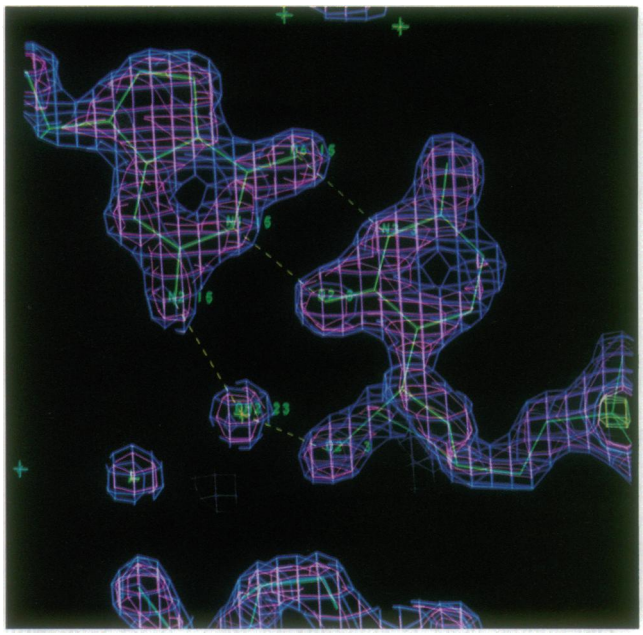

FIG. 1. Electron density map at 1.6-Å resolution with superimposed atoms for the U^3·G^{15} base pair. The well-defined water molecule seen in the map provides additional stabilization of the base pair through hydrogen bonding to O2′ of U^3 and N2 of G^{15}. The base pair G^6·U^{12} is virtually identical.

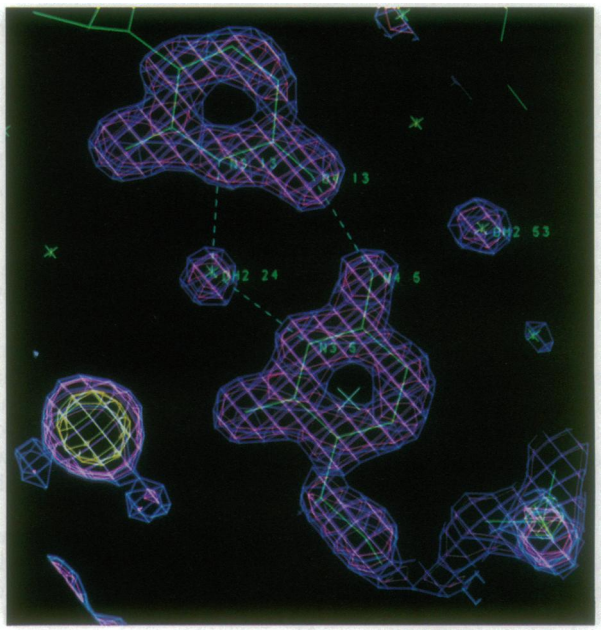

FIG. 2. The C^5·U^{13} base pair superimposed on the electron density map at 1.6-Å resolution. A hydrogen bond (2.81 Å) is formed between O4 of U^{13} and N4 of C^5. The bases are also linked through hydrogen bonds to a bridging water molecule seen here. The second C·U pair is virtually identical. Note the hexamminerhodium cation, which is coordinated to O2 of C^5.

evidence for its involvement as a mechanism for errant pairing during the propagation of genetic information *in vivo*. Substitutions that introduce G·U (and G·T) pairs in oligonucleotides lead to destabilizations which are small compared with other mismatches as measured by the effect on the midpoint of the thermal denaturation curve. The difference is particularly small in RNA duplexes.

Ordered water molecules in hydrogen-bonding contact with functional groups not directly involved in base-pair formation contribute to stability. They have been observed in all published G·U- or G·T-containing structures. Such water molecules can be seen clearly in Fig. 1. In the present structure, as in the RNA dodecamer, the 2′-hydroxyl group participates in the network connecting O2′(U) to N2(G) through an intermediate water molecule. In oligodeoxynucleotides an analogous bridge is formed between O2 and N2 of the same residues.

C·U Mismatch. Classically, speculations on the mechanism of base pairing between pyrimidines have led to structures of limited compatibility with standard double-helix geometry, a hypothesis which seemed to be supported by the poor crystallinity of such mismatch-containing sequences. The present, high-resolution structure demonstrates a configuration of the C·U pair that can be accommodated in an A-RNA duplex with only minor distortions. In Fig. 2, one of the C·U base pairs is superimposed on the electron density map at 1.6-Å resolution. The other C·U pair is virtually identical. Both bases are in the major tautomer forms. A direct hydrogen bond of 2.81 Å links O4(U^4) and N4(C^{14}) (2.78 Å in the U^{13}·C^5 base pair). The N3 atoms are hydrogen-bonded to the same well-localized water molecule, at distances of 2.88 Å and 2.82 Å (corresponding values, 2.68 Å and 2.87 Å). This arrangement stabilizes the pyrimidine–pyrimidine base pair while at the same time it separates the O2 atoms and allows the glycosidic bonds to assume orientations similar to those of a Watson–Crick base pair (Table 1). There is little stacking overlap between adjacent base pairs in this region of the duplex.

Extended Crystal Structure and ^{Br}U·^{Br}U Pairing. In the extended crystal structure the duplex fragments are related by twofold axes at 0,0,½ and 0,0,0 to form continuous double helical stacks parallel to the *c* axis (Fig. 3). Different stacking interactions are utilized at the two ends of the molecule. At 0,0,½ contact occurs with stacking between the terminal C^8·G^{10} base pair of the octamer core and that of its symmetry-related neighbor. $^{Br}U^9$ does not participate in this stacking but occupies the minor groove of the symmetry-related duplex (represented by *) (Fig. 4).

There are two close contacts between the deoxyribose ring and this duplex: a hydrogen bond between O4′($^{Br}U^9$) and O2(C^{11*}) (2.61 Å) and another between O3′($^{Br}U^9$) and N2(G^{7*}) (3.18 Å). There is a further hydrogen bond (2.71 Å), between N3($^{Br}U^9$) and the phosphate oxygen atom of the symmetry-related duplex displaced by one cell translation along the short *b* axis, O1($U^{3*''}$). Additional cohesion is provided in this region by the Rh^{22} cation, which is coordinated to one phosphate oxygen from each of the duplexes in adjacent cells. The distances are as follows: O1P(U^{12*})—N3(Rh^{22}), 2.77 Å; O1P($U^{3*''}$)—N6(Rh^{22}), 2.50 Å. Rh^{22} is also linked to O4 of $^{Br}U^9$ (2.97 Å). The coordination is completed by a water molecule, W^{32}, 2.58 Å from N6(Rh^{22}) and 2.85 Å from N2(Rh^{22}).

At the other end of the duplex, consecutive molecules are related by the twofold axis at the origin of the cell with the G^1·C^{17} and G^{1*}·C^{17*} base pairs separated by ≈6.5 Å. This region is disordered. The terminal base $^{Br}U^{18}$ occupies two alternative intrahelical positions, $^{Br}U^{18a}$ and $^{Br}U^{18b}$. Hydrogen-bonded pairs are formed between bases of symmetry-related molecules; $^{Br}U^{18a}$ pairs with $^{Br}U^{18b*}$ and $^{Br}U^{18b}$ with $^{Br}U^{18a*}$. The hydrogen-bond distances are 2.6 Å between N3 and O2 and 2.5 Å between O4 and N3. These base pairs provide continuity of stacking between the helices along the *c* axis. The geometry of the T·T base pairs is compatible with the requirements of the sugar-phosphate backbone of a double helix.

Fig. 5 shows the electron density around the origin of the unit cell. It is an "omit" map with the contribution of $^{Br}U^{18}$ omitted from the calculation. Although the structure is clearly disordered in this region, the positions of two (disordered) bromine atoms are well defined. These, together with

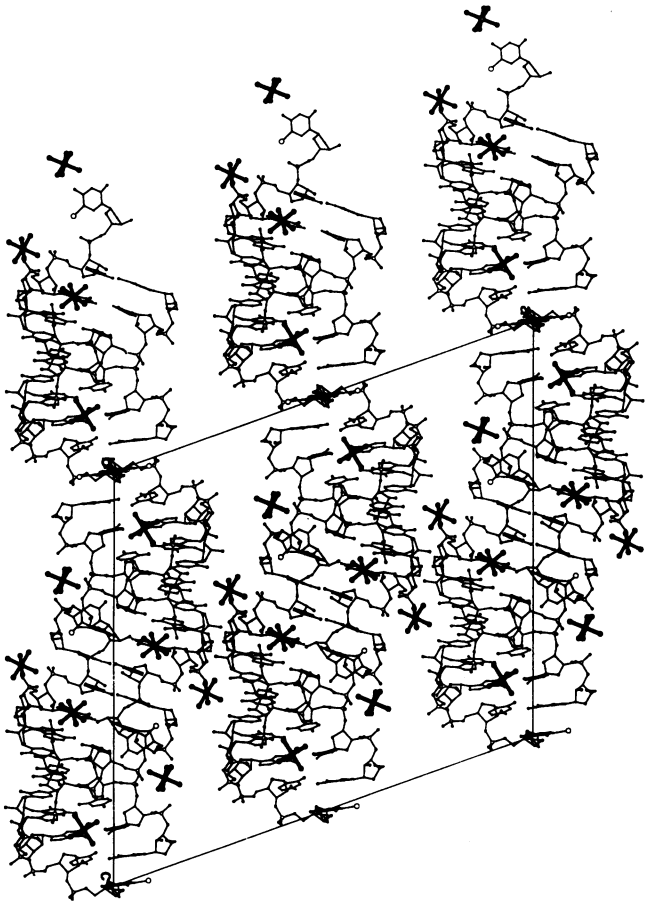

FIG. 3. A view of the extended crystal structure projected on the *ac* plane and showing the infinite columns of stacked double helices along the *c* axis. The four hexamminerhodium cations (ball and stick drawings) located in the analysis are also shown.

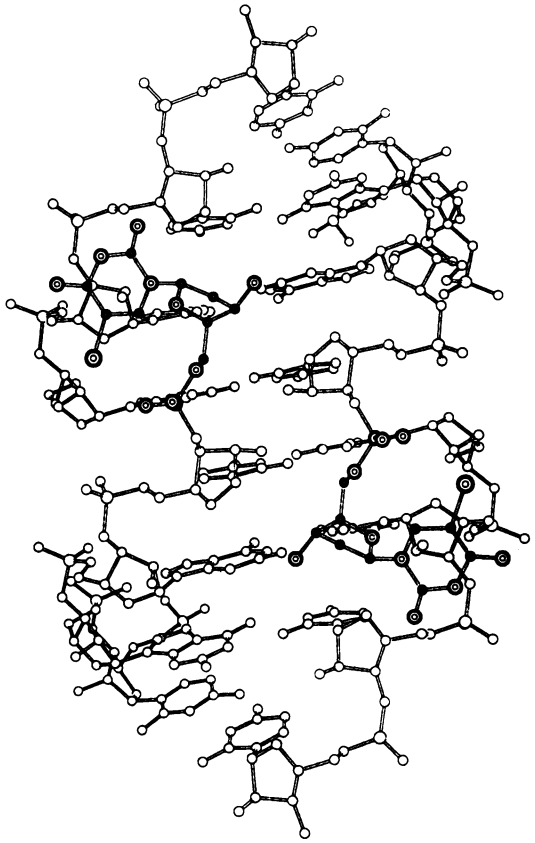

FIG. 4. Stacking of terminal base pairs of two symmetry-related double helices around the twofold axis at 0,0,½. The bromouracil bases of $^{Br}U^{9}$ and $^{Br}U^{9*}$ (drawn darker) are rotated away from the helical core into the minor groove and form a number of hydrogen bonds as described in the text.

the phosphate groups of the backbone and localization of the base planes in van der Waals contact with their neighbors, allow the orientation of the pyrimidine rings to be determined unambiguously as shown in Fig. 5, where the $^{Br}U{\cdot}^{Br}U$ base pairs are superimposed on the electron density map. It should be remembered, however, that the backbone is discontinuous at this point, and that local disorder leads to high standard deviations in the atom positions.

The disorder observed in this structure is clearly a consequence of the absence of twofold symmetry of the $^{Br}U{\cdot}^{Br}U$ base pair that is required at this position in the unit cell. The symmetry of the molecular environment is incapable of distinguishing the two possible orientations of the base pairs, which were assigned equal occupancy in the refinement. The two orientations presumably reflect optimal stacking between the terminal C·G pairs.

The parallel helical columns are linked by elaborate networks of ions and solvent molecules, only some of which can be located uniquely.

The Counterions. Hexamminerhodium cations play an important role in maintaining the ordering of the molecules in the crystals. These cations are at four principal sites: Rh^{19} (B = 11 Å^2) and Rh^{20} (B = 14 Å^2) are at two fully occupied sites where the nitrogen ligands are fully located, while the Rh^{21} (B = 14 Å^2) and Rh^{22} (B = 16 Å^2) sites have occupancies of 35% and 30%, respectively.

Rh^{19} is in the major groove coordinated to the O2P atoms of C^5 (2.71 Å) and G^6 (2.94 Å) and to the O6 atoms of G^6 (2.78 Å) and G^7 (3.02 Å). The coordination sphere also includes a water molecule at 2.93 Å. Rh^{21} is in the corresponding position of strand 2, coordinated to G^{16} and G^{17} and two water molecules. However, the contacts made by the two cations are not identical, which might well account for the change in backbone orientation at this point, noted in an earlier section.

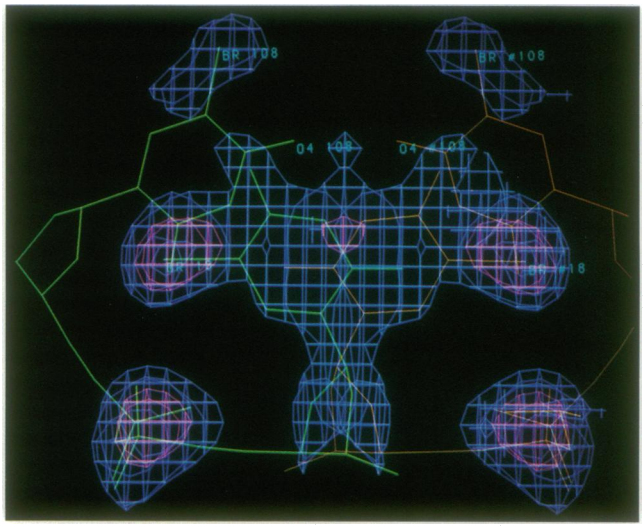

FIG. 5. The $^{Br}U{\cdot}^{Br}U$ base pairs superimposed on the electron density "omit" map in the neighborhood of the origin, 0,0,0. This region of the structure is disordered with the $^{Br}U^{18a}{\cdot}^{Br}U^{18b*}$ and the $^{Br}U^{18a*}{\cdot}^{Br}U^{18b}$ base pairs in two alternative orientations. The positions of the bromine atoms are well defined and, together with the plane of the pyrimidine rings, which fit into a clear region of electron density, serve to locate the positions of the base pairs.

Rh^{20} is in a channel between adjacent duplexes with numerous intermolecular contacts. Rh^{22} is in a cavity close to $^{Br}U^{9}$ and participates in interactions between the parallel stacks of helices.

DISCUSSION

Selectivity in base pairing is central both to the mechanisms which transfer and express genetic information and to maintaining the secondary structures of nucleic acids. The near-exclusive preference for pairing between A and T or U and between C and G is well established in transcription and especially replication, where selectivity afforded by optimal hydrogen bonding is enhanced by other more complex mechanisms that contain mutation rates within tolerable limits. Recognition of non-Watson–Crick base pairs in the DNA double helix that must precede repair of these lesions appears to depend on structural properties more than on duplex stability (13). Three mismatches are observed in the nonamer duplex. Although the duplex is of the A form, the essential geometry of the base pairs is interchangeable with B-DNA (Fig. 6).

The C·U pairs, which have no counterparts in DNA crystal structures, are seen here only for the second time within a double helix. Participation of a water molecule, as an integral component of the hydrogen bonding between the bases, widens the base pair to almost standard proportions. The symmetric distribution of the glycosidic bonds also resembles that of a Watson–Crick base pair and is a property that has been related to the efficiency of mismatch repair in DNA (14). C·T is a poor substrate for the repair system in bacteria (13), and the model observed here is, therefore, consistent with the hypothesis.

There are no examples of T·T pairs in solid-state structures of duplexes, but the ^{Br}U·^{Br}U pair is directly analogous and can be considered to some extent intrahelical since it forms part of the continuous column of stacked duplexes. These terminal nucleotides are conformationally less restricted than others within the body of the duplex, but compatibility with extended structures of this type can be assessed from the distance between the anomeric carbons and the relative orientations of the glycosidic vectors. The parallel is reinforced by early NMR studies in solution on a duplex containing T·T pairs: despite destabilization of the duplex, the two bases formed part of the helical stack and a wobble pair of the present type was inferred (15).

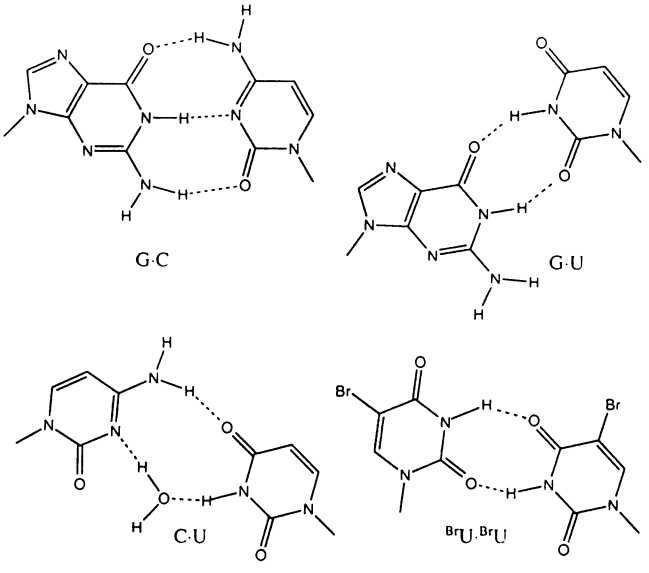

FIG. 6. Comparison of the noncanonical base pairs observed in this analysis with the Watson–Crick G·C pair.

Both the present structure and the dodecamer (8) contain the sequence r(UUCG). Such sequences are known in solution to produce tetraloops of high thermal stability (16) which might be regarded as an intrinsic structural property of this sequence. In the crystal, however, both oligomers form duplexes with four adjacent U·G and U·C pairs. There appear to be no specific inter- or intramolecular interactions that conspicuously favor mismatches in either structure, nor can these pairs be attributed to the influence of the hexammine-rhodium cations, which were present only in the nonamer. The collection of mismatches in these structures must, therefore, be due to the crystal environment that stabilizes the duplex as a whole. It is clearly also the crystal environment that fortuitously leads to self-pairing of ^{Br}U. Our results thus have an important bearing on the difference between solution and crystal structures. Both loops and helices are features of various forms of RNA, and the stable base-pair mismatches observed in crystals need to be taken into account in analyzing and predicting RNA secondary structures.

We thank Dr. S. R. Holbrook for supplying the coordinates of the dodecaribonucleotide, Dr. R. Fourme and Dr. R. Kahn for the anomalous data recordings at Lure, the Medical Research Council Laboratory for Molecular Biology for data collection facilities, Dr. C. M. Nunn for her contribution to the early stages of this project, and Mr. B. L. Partridge for help with the preparation of diagrams. We are particularly grateful to Dr. S. A. Salisbury for his help with the analysis of the results and the preparation of the manuscript. The work was supported by a Medical Research Council Program Grant (to O.K.).

1. Chastain, M. & Tinoco, I. (1991) *Prog. Nucleic Acid Res. Mol. Biol.* **41**, 131–178.
2. Kim, S. H., Suddath, F. L., Quigley, G. J., McPherson, A., Kim, J. J., Sussman, J. L., Wang, A. H.-J., Seeman, N. C. & Rich, A. (1974) *Science* **185**, 435–439.
3. Robertus, J. D., Finch, J. T., Rhodes, D., Brown, R. S., Clark, B. F. C. & Klug, A. (1974) *Nature (London)* **250**, 546–551.
4. Moras, D., Comarmond, M. B., Fischer, J., Weiss, R., Thierry, J. C., Ebel, J. P. & Giegé, R. (1980) *Nature (London)* **288**, 669–674.
5. Jeger, J. A., Turner, D. H. & Zuker, M. (1989) *Proc. Natl. Acad. Sci. USA* **86**, 7706–7710.
6. Heus, H. A., Pardi, A. & Turner, D. H. (1991) *Science* **253**, 191–194.
7. Varani, G., Cheong, C. & Tinoco, I. (1991) *Biochemistry* **30**, 3280–3289.
8. Holbrook, S., Cheong, C., Tinoco, I. & Kim, S.-H. (1991) *Nature (London)* **353**, 579–581.
9. Navaza, J. (1990) *Acta Crystallogr. Sect. A* **46**, 619–620.
10. Doucet, J., Benoit, J., Cruse, W. B. T., Prangé, T. & Kennard, O. (1989) *Nature (London)* **337**, 190–192.
11. Brunger, A. (1992) X-PLOR Manual (Yale Univ., New Haven, CT), Version 3.0.
12. Kennard, O. & Salisbury, S. A. (1993) *J. Biol. Chem.* **268**, 10701–10704.
13. Modrich, P. (1987) *Annu. Rev. Biochem.* **56**, 435–466.
14. Hunter, W. N., Brown, T., Anand, N. N. & Kennard, O. (1986) *Nature (London)* **320**, 552–555.
15. Cornelis, A. G., Haasnoot, J. H. J., den Hartog, J. F., de Rooij, M., van Boom, J. H. & Altona, C. (1979) *Nature (London)* **281**, 235–236.
16. Woese, C. R., Winkler, S. & Guttell, G. (1990) *Proc. Natl. Acad. Sci. USA* **87**, 8467–8471.